**Proceedings of the ASME 2015 International Technical Conference and Exhibition on Packaging and Integration of Electronic and Photonic Microsystems and
ASME 2015 13th International Conference on Nanochannels, Microchannels, and Minichannels
InterPACKICNMM2015
July 6-9, 2015, San Francisco, California, USA**

InterPACK/ICNMM2015-48499

PASSIVE THERMAL MANAGEMENT USING PHASE CHANGE MATERIALS: EXPERIMENTAL EVALUATION OF THERMAL RESISTANCES

Yash Ganatra
Amy Marconnet
Purdue University
West Lafayette,
Indiana - 47907

ABSTRACT

Limited heat dissipation and increasing power consumption in processors has led to a utilization wall. Specifically due to high transistor density, not all processors can be used continuously without exceeding safe operating temperatures. This is more significant in mobile electronic devices which, despite relatively large chip area, are limited by poor heat dissipation - primarily natural convection from the exposed surfaces. In the past, solid-to-liquid phase change materials (PCMs) have been employed for passive thermal control – absorbing energy during the phase change process while maintaining a relatively fixed temperature. However, the lower thermal conductivity of the liquid phase after melting often limits the heat dissipation from the PCM, and in the liquid state, the material can flow away from the desired location. Here we focus on characterization of thermal performance of PCMs with the goal of evaluating dry (gel-to-solid/amorphous-to-crystalline) phase change materials which are intended to mitigate the pumpout issue. Critical thermophysical properties include the thermal conductivity, heat capacity, and latent heat of the phase/state change. The thermal resistance throughout the phase change process is measured by in-house rig which miniaturizes the reference bar method for use with infrared temperature sensing.

INTRODUCTION

Consumer electronics are now characterized by increasing integration of advanced features leading to increased performance and compactness, especially for smartphones. This has resulted in significant increase in power density, in turn leading to higher temperatures inside the device. The need for an efficient thermal management system is two-fold – (1) thermal limits such as the case (surface) [1], silicon die, DRAM, and battery temperatures remain unchanged and (2) the increased failure rate of electronic devices at higher operating temperatures [2]. In 1989, a survey by the US Air Force illustrated that more than half of electronics failures were related to thermal issues (as more recently described in a review article [3] on electronics cooling technologies). This high thermal-driven failure rate highlights the need to develop new thermal management solutions to reduce failure and meet performance scaling trends. Beyond complete failure, device performance can suffer at elevated temperatures: transistor gate leakage current increases exponentially with temperature [4].

Cooling techniques can be divided into two categories – active and passive. Active cooling entails the use of forced convection via fans, liquid cooling through microchannels [5] micronozzles [8], heatpipes [9] and thermoelectric cooling [10]. Passive cooling techniques use a combination of heat spreaders, thermal interface materials and thermal vias to move and store the heat within the device. Size and weight constraints in embedded or mobile systems can preclude the use of active cooling techniques, ensuring that all generated power must be dissipated by natural convection and radiation from the case. This limitation imposes restrictions on device performance often meaning that only a fraction of transistors are active at a given time. Runtime thermal management techniques, which monitor thermal behavior, optimize operating parameters of processor, and predict temperatures, have emerged as a consequence of this thermal bottleneck [12].

Copyright © 2015 by ASME

Thermal interface materials (TIMs) are often fabricated from low thermal conductivity polymers infiltrated with high thermal conductivity fillers. Low manufacturing costs and increased robustness of semiconducting polymers has made them a promising technology [15] and inorganic polycrystalline polymers have received much emphasis, especially semiconducting polymers which have improved charge transport characteristics compared to most polymers. Additionally, recent work has shown that highly disordered or amorphous polymers perform as well as semicrystalline materials for photovoltaic applications [16]. The increased electrical performance of all of these materials compared to conventional polymers could also yield improved thermal properties making them intriguing for thermal applications. Noriega *et al.* [18] developed a unifying framework for charge transport which can also influence thermal transport. Bulk polymers generally have low thermal conductivity on the order of $0.1\,W\,m^{-1}K^{-1}$ [19]. But recent work has reported high thermal conductivities in individual nanofiber of polyethylene of order of $100\,W\,m^{-1}K^{-1}$, which is higher than many metals [20]. If the high thermal conductivity of the individual molecular chains that form the backbone of many polymers could be exploited in a more bulk format, polymers could prove useful as thermal interface materials.

Traditional TIMs are designed to fill the gaps between heat sink and chip thus reducing contact resistance. For passive thermal management applications, we consider polymers which undergo a gel-to-solid or amorphous-to-crystalline molecular state transition upon heating and cooling allowing energy to be absorbed through the latent heat of phase change, without pumpout and other issues associated with PCMs that melt. Furthermore, these materials are particularly interesting for passive thermal management because the high temperature state may have higher thermal conductivity. Thus, heat could be removed effectively during the state transition due to the enthalpy of phase change and continue to be transported effectively at the higher temperature state.

Future work will include (1) measuring the heat capacity and latent heat using differential scanning calorimetry (DSC); and (2) investigation of the feasibility of integrating these novel PCMs into chip stacks by using a heater to mimic the power dissipation rates expected for smartphone processors. Here we focus only on the thermal conduction through the material at different temperatures.

BACKGROUND

Research on thermal systems has focused on transient thermal management due to temporal variation of workloads at the device level and generation of local hotspots at chip scale. Phase Change Materials (PCMs) which store and release energy during melting and freezing were first used in space applications [22]. Sharma *et al*. [24] recently reviewed the use of PCMs in latent thermal energy storage with an emphasis on applications like solar water-heating systems and building heating/cooling. But the same materials are attractive for electronics thermal management and several groups have numerically and experimentally evaluated methods for integrating PCMs into electronics cooling.

Several approaches have been developed to quantify the effectiveness of integrating PCMs in electronics cooling. Key metrics include temperature stability and the ability to accommodate repeated transient heating events. Beyond thermal storage properties, the thermal conductivity of the PCM impacts the effectiveness of integrating the PCM into the cooling scheme. Specifically, Joshi *et al*. [26] compared metallic and organic PCMs at varying power levels and determined low thermal conductivity of organic PCMs causes only a fraction of heat dissipated by the module to be absorbed by the PCM. Thus, they recommended metallic PCMs for the primary heat flow path. Often, due the physical dimensions of the system, natural convection effects, which could enhance heat dissipation, are generally negligible. But Chebi *et al.* [25] designed phase change systems to take advantage of buoyancy-driven natural convection in the melted PCM to enhance heat transfer rates.

Highly conductive extended surfaces, fins [27], and honeycomb structures [29] have been used in conjunction with organic PCMs. Wirtz *et al*. [32] proposed use of solid-solid phase change integrated into a finned heat sink developing a thermal resistance network model including the fin, the adjacent PCM and convection heat transfer to the ambient from the exposed portion of fin. The authors defined a figure of merit for the hybrid cooler in terms of the stabilization and recovery time during heating and cooling. Amon and colleagues [30-31] numerically evaluated the performance aluminum honeycomb structures (with high thermal conductivity) filled with PCMs for wearable electronics over several cycles of heating. A major outcome of their work involved developing metrics for quantifying the performance including the efficiency η (*i.e.* the percentage of energy stored in the system during phase change compared to the total heat transferred to the system), the temperature fluctuation band, T_{band} that quantifies the temperature stability during cycling, and the peak energy storage ψ that quantifies how the system responds to a burst in thermal energy.

System thermal analysis involves analyzing heat flow paths from the heat source to the ambient in an electronic device and often results in modeling different components as thermal resistance networks. PCMs are modeled as capacitance in these system analyses. Hodes *et al*. [33] investigated the feasibility of incorporating PCMs in a portable handset using a Kapton® heater to mimic heat generated by a chip and measured times for the PCMs to reach various temperatures and recharge. This work highlights one challenge in implementing this approach: while the PCMs help delay spikes in temperature, once melted, the re-solidification of these configurations required 10-30 minutes. The experimental results were compared with simulations accounting for radiation heat transfer and uncertainties introduced due to heat conduction through thermocouples. Cho *et al*. [35] embedded a heater in a mobile phone to mimic a processor and showed that conduction is the dominant mode of heat transfer in a mobile

Copyright © 2015 by ASME

phone by measuring excess temperature over ambient of different components (keyboard, PCB and battery). The variation in the in-plane and cross-plane thermal conductivities was also considered. To prevent overheating, the authors recommended almost equal power dissipation through the keyboard (upper end) and the battery (lower end). Tso *et al.* [36] experimentally investigated the use of PCM in aluminum heat sink with varying number of fins at different power levels and usage conditions. They concluded that the duration of usage should be within the time needed to melt the PCM because time taken for re-solidification is significantly longer than time taken to melt.

At the chip scale, Gurrum *et al.* [34] simulated and experimentally investigated the impact of incorporating metallic PCMs in microchannels during periodic power cycling. Variation of the channel width, proximity of the PCM to the heat source, and the effect of adding a diamond heat spreader was considered. The effective thermal conductivity of PCMs embedded in SiC microchannels was higher than a stacked arrangement of SiC and PCM. The thermal conductivity of the PCM and sidewalls affected the effectiveness of PCM which was shown by the increase in temperature decrease at high power densities when diamond heat spreader was used.

Raghavan *et al.* [37] proposed computational sprinting where thermal design power (TDP) is exceeded in short bursts by turning on all available cores at highest voltage/frequency setting until a threshold temperature is reached to improve responsiveness using PCM. The package and the PCM were represented as resistances and capacitances and thermal modeling was done for 16W sprint on a 1W TDP system. The authors showed that the sprinting could be sustained for 1s and the re-solidification time was 20s. In addition to the passive thermal management applications, solid-liquid PCMs find use as a Thermal Interface Material (TIM) due to their ability to conform to surfaces after melting [39].

In short, simulations and experiments have demonstrated that integrating PCMs into electronics cooling systems can allow increased computational performance while stabilizing temperature in the system. However, materials properties including thermal conductivity in the low and high temperature state, the latent heat of phase change, and heat capacity contribute to performance. Furthermore, different integration schemes for including PCMs may require different materials.

Table 1 Dimensions and material properties of thermal conductivity rig components

Component	Material	Dimensions (L x B x H) (mm)	Thermal Conductivity (W/mK)	Density (kg/m^3)
Adapter plate	Copper	40 x 40 x 3	390	8900
Cooling system plate	Copper	40 x 40 x 10	390	8900
Heater plate	Copper	60 x 40 x 6	390	8900
Insulation Plate	MACOR®	80 x 45 x 14	1.46	2520
Reference	Fused Silica	10 x 10 x 1.5	1.4	2201

EXPERIMENTAL PROCEDURES

In the conventional reference bar method [40], an unknown sample is sandwiched between long bars of a known reference material. Several thermocouples are placed along the length of the reference material to measure the heat flux through the sample and the measured temperature gradient is extrapolated to the sample location to estimate the thermal conductivity or total thermal resistance of the sample. For a single sample, it is impossible to separate the contact resistance from the intrinsic sample thermal conductivity and often several thicknesses of "identical" samples are measured to separate out these two effects.

In contrast, the miniature infrared (IR) reference bar method (see **Table 1**, **Figure 1**, and **Figure 2**) used in this work

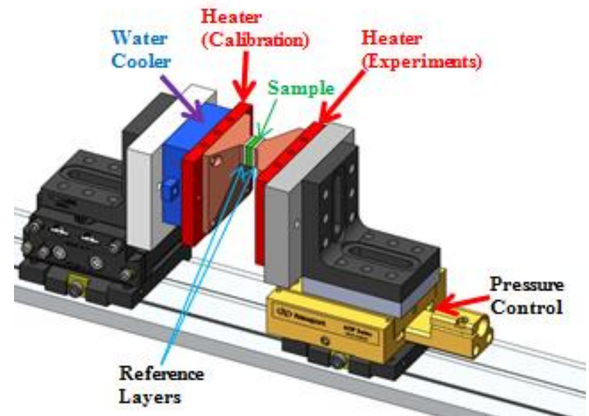

Figure 1 Schematic of the miniature IR thermal conductivity measurement rig.

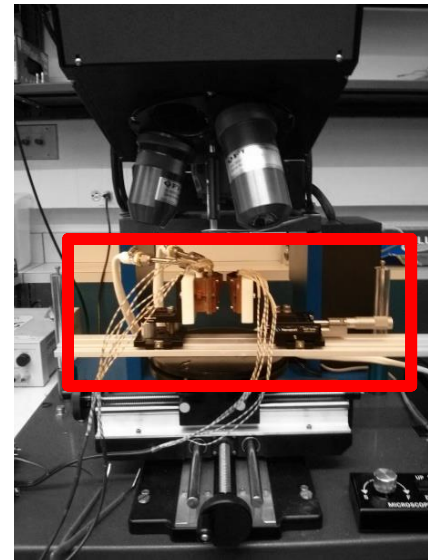

Figure 2. Miniature IR thermal conductivity measurement rig mounted on IR microscope stage. The components of thermal conductivity rig (in color and enclosed by red outline) are shown in Figure 1.

Copyright © 2015 by ASME

non-invasively measures two-dimensional temperature maps across the entire reference-sample reference stack. Compared to the conventional method, the reference layers are much thinner (~ 1 mm) and the material for the reference layer is chosen to have a thermal resistance (R" = L/k in cm^2 K/W) on the same order of the sample. A high spatial (1.7 μm/pixel to 11.7 μm/pixel) and temperature (~0.1 K) resolution IR microscope (Quantum Focus Instruments) records the two-dimensional temperature map when a heat flux is passing through the sample and the thermal conductivity of the sample (reflected in the temperature gradient within the sample) can be spatially separated from interface effects (which appear as temperature jumps at boundaries between materials). [41-42]

In this method, the sample is sandwiched between fused silica reference layers forming the Reference-Sample-Reference. Two reference layers are required to quantify the heat flux and accurately account for heat losses to the surroundings. To prevent sample contamination, no coating is applied on the surfaces. Cartridge heaters (Watlow® Firerod C1J5) embedded in copper heater plates on either side of the Reference-Sample-Reference stack heat the sample stack to a uniform temperature during emissivity calibration. For calibration, the Reference-Sample-Reference stack is heated from both sides to 40ºC, which is less than the melting point of the samples. A reference radiance image is taken which compares the radiance at each pixel with a blackbody at the same temperature. This corrects for non-ideal emissive properties of the surface, accounts for variations in the surfaces of the sample, and allows measurement of multiple materials with different emissivities in one image. High thermal conductivity copper adapter plates taper from the large cross section heater plate to the smaller cross-section of the sample to ensure one-dimensional heat transfer through the sample stack as shown in **Figure 2**. Future work will include geometry optimization of the adapter plates to minimize cross plane temperature variation. After calibration, the cooling system is switched on and maintains the cold side temperature at ~24°C, while the heater power to the other side is adjusted to establish the desired temperature differential. The measurement is repeated at several different applied powers, and the thermal conductivity and interface resistances are extracted from the power-dependent results. Phase change is also recorded by movies of the temperature and radiance maps. This entire measurement rig is supported by two linear stages to accommodate samples of different sizes and allow variations in the pressure applied across the sample. The stages are isolated from the heated and cooled regions using Macor ® insulation.

Since heat flow is one-dimensional across the Reference-Sample-Reference stack, the thermal conductivity of the sample is determined by computing the heat flow across the three layer stack [43]. For uniform cross-sectional areas, the relationship between the temperature gradient in each layer *i* and temperature jumps at an interface are given by

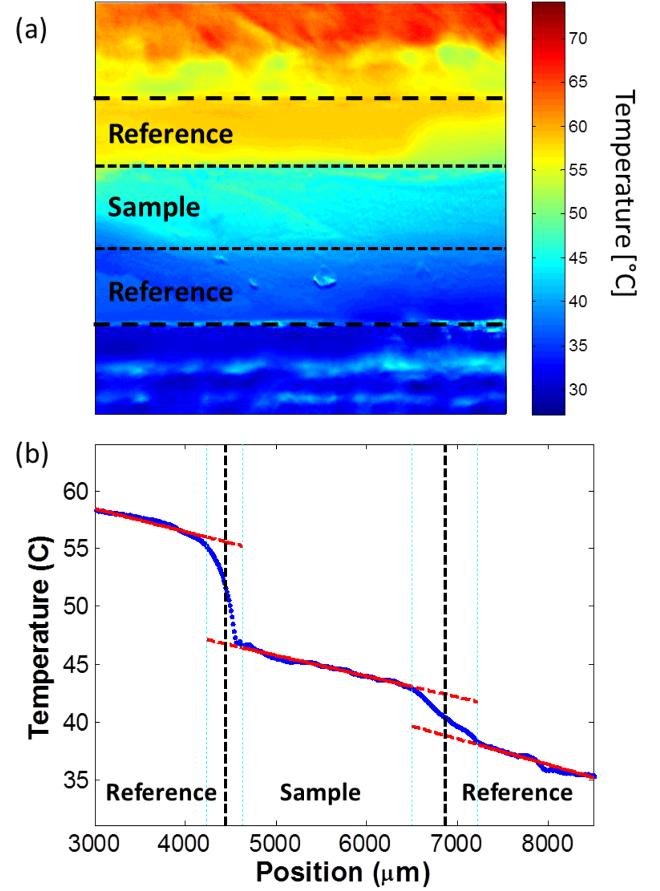

Figure 2 (a) Two dimensional temperature map and (b) the averaged one-dimensional temperature profile for a cross section of TIM sample between two reference layers. Temperature jumps at interfaces are clearly visible in the averaged temperature profile in addition to the linear region in the sample region. Thus, the interface resistances can be spatially separated from the thermal conductivity of the sample.

$$q_i'' = -k_i \frac{dTi}{dx} = \frac{\Delta T_{int}}{R_{int}''}, \tag{1}$$

where q_i is heat flux in *x*-direction, k_i is thermal conductivity, dTi/dx is temperature gradient in i^{th} layer, ΔT_{int} is the temperature jump at an interface, and R_{int}'' is the thermal resistance of the interface (m^2 K /W). Thus, the ratio of the thermal conductivities of the sample and reference regions related to the temperature gradients in each region as:

$$\frac{k_{sample}}{k_{ref}} = \frac{\left(\frac{dT}{dx}\right)_{ref}}{\left(\frac{dT}{dx}\right)_{sample}}, \tag{2}$$

and interface resistances can be calculated from

$$R_{int}'' = \frac{\Delta T_{int}}{-k_{ref}\left(\frac{dT}{dx}\right)_{sample}}. \tag{3}$$

Figure 2 shows an example temperature map and 1-D averaged temperature profile for an average sample temperature near 45ºC for a commercial phase change thermal interface

Copyright © 2015 by ASME

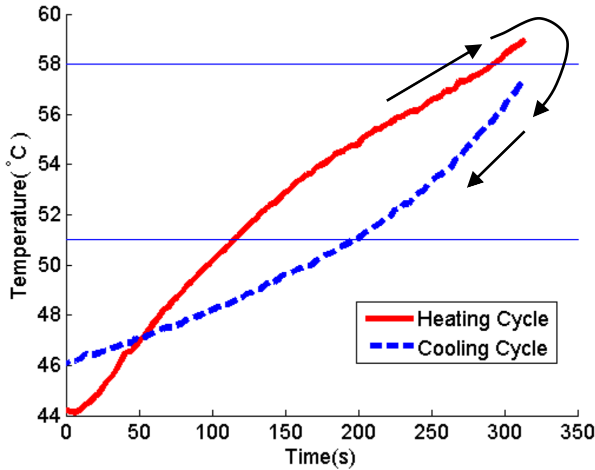

Figure 3 Temperature history of T766-06 TIM. The mean temperature of a small region of interest around the center of the sample is plotted with time. During heating, phase change occurs over a range of temperatures (51-58 ºC) as indicated by blue reference lines, but during cooling the impact of phase change is not as obvious indicating the freezing temperature depressed. Arrows indicate that after the sample was fully heated the material was subsequently cooled.

material (Chromerics Thermflow™ T766-06) [44] which has phase change temperature range from 51-58 ºC. The sample contains a non-adhesive metal foil carrier on one face which faces the heater and the adhesive PCM faces the water cooling system. In **Figure 2**, the sample is still completely solid and has not experienced phase change. From these temperature maps, a total thermal resistance of the TIM ($R''_{tot} = R''_{int,hot} + \frac{L}{k} + R''_{int,cold}$) of 13 cm^{2}K/W (in the solid state) can be extracted and separated into three components: the PCM material with an intrinsic thermal conductivity of 0.3 W/(m K) and interface resistances of $R''_{int,hot} = 0.30$ and $R''_{int,cold} =$ 6.19 cm^{2}K/W. Additionally, two-dimensional effects can be observed through the variations in temperature along each vertical column of pixels due to non-uniformities in the sample and contact conditions.

Upon further heating of the hot side, melting occurs in a localized manner around "hot spots" with temperatures greater than melting temperature along the sample-reference interface on the hot side. **Figure 3** shows the evolution of the temperature profile using two different cycles which is tracked by recording using the movie mode in IR-Microscope. For the heating cycle, initially, the heater power is raised such that temperature exceeds the phase change temperature range, after which the heater is switched off (cooling cycle).

The variation of thermal resistance during these cycles is summarized in **Table 2**. The effective thermal resistance is reduced during phase change (compared to when the sample is fully solid). Also, after fully melting the thermal resistance is reduced by ~50% and remains at this reduced value throughout cooling. This is due to improved contact at the interfaces of the TIM after melting that persists even during resolidfication, as well as a reduced bond line thickness. Spatially varying temperature gradients in the sample induce stresses which often lead to pump out of the thermal interface material after melting. After resolidification, the thickness of the TIM remaining in between the two reference layers has reduced such that the film remaining is semi-transparent (as compared to a fully opaque layer before testing). This result highlights the need to control and confine the sample during the melting and re-solidification process, as well as a potential advantage of the dry PCMs which never fully liquefy.

Table 2 Thermal Resistance (in cm^{2}K/W) for heating and cooling cycles for temperatures between and below (solid state) phase change temperature range

Cycle	During phase change	Solid
Heating	11.031	13.143
Cooling	6.6501	6.6425

SUMMARY AND CONCLUSIONS

This work highlights a testing method developed to characterize performance of dry PCMs for thermal management applications. Namely a miniaturized infrared microscopy version of the standard reference bar method is presented as a compact system for evaluating thermal resistance and phase change behavior of these complex systems. Preliminary results for a commercially available phase-change thermal interface material demonstrate the efficacy of the technique and illustrate that pump out of conventional PCMs which melt is a major issue. Measurements of the dry phase change materials are under way and will yield useful inputs for models enabling design of electronic systems with dry PCMs for passive thermal management.

ACKNOWLEDGEMENTS

This work is supported by the Cooling Technologies Research Center, an NSF I/UCRC center at Purdue University. The contribution of undergraduate students, Michael Woodworth and Claire Lang is gratefully acknowledged.

REFERENCES

[1] T. E. Bernard and M. F. Foley, "Upper acceptable surface temperature for prolonged hand contact," *Int. J. Ind. Ergon*., vol. 11, no. 1, pp. 29–36, 1993.

[2] P. Mithal, "Design of experimental based evaluation of thermal performance of a flipchip electronic assembly," *ASME EEP Proceedings*. New York ASME, vol. 18, pp. 109–115, 1996.

[3] L.T. Yeh, "Review of heat transfer technologies in electronic equipment," *J. Electron. Packag*., vol. 117, no. 4, pp. 333–339, 1995

Copyright © 2015 by ASME

[4] A. Shakouri, "Nanoscale thermal transport and microrefrigerators on a chip," *Proc. IEEE*, vol. 94, no. 8, pp. 1613–1638, 2006
[5] R. Hannemann, J. Marsala, and M. Pitasi, "Pumped liquid multiphase cooling," in ASME 2004 *International Mechanical Engineering ongress and Exposition*, 2004, pp. 469–473
[6] J. Lee and I. Mudawar, "Two-phase flow in high-heat-flux micro-channel heat sink for refrigeration cooling applications: Part I—pressure drop characteristics," *Int. J. Heat Mass Transf.*, vol. 48, no. 5, pp. 928–940, 2005
[7] J. Lee and I. Mudawar, "Low-temperature two-phase micro-channel cooling for high-heat-flux thermal management of defense electronics," in *Thermal and Thermomechanical Phenomena in Electronic Systems*, 2008. ITHERM 2008. 11th Intersociety Conference on, 2008, pp. 132–144
[8] C. H. Amon, J. Murthy, S. C. Yao, S. Narumanchi, C.-F. Wu, and C.-C. Hsieh, "MEMS-enabled thermal management of high-heat-flux devices EDIFICE: embedded droplet impingement for integrated cooling of electronics," *Exp. Therm. Fluid Sci.*, vol. 25, no. 5, pp. 231–242, 2001
[9] H. Xie, A. Ali, and R. Bhatia, "The use of heat pipes in personal computers," in *Thermal and Thermomechanical Phenomena in Electronic Systems*, 1998. ITHERM'98. The Sixth Intersociety Conference on, 1998, pp. 442–448
[10] G. J. Snyder, M. Soto, R. Alley, D. Koester, and B. Conner, "Hot spot cooling using embedded thermoelectric coolers," in *Semiconductor Thermal Measurement and Management Symposium*, 2006 IEEE Twenty-Second Annual IEEE, 2006, pp. 135–14
[11] S. Biswas, M. Tiwari, T. Sherwood, L. Theogarajan, and F. T. Chong, "Fighting fire with fire: modeling the datacenter-scale effects of targeted superlattice thermal management," in *Computer Architecture (ISCA)*, 2011 38th Annual International Symposium on, 2011, pp. 331–340
[12] C.-H. Chao, K.-Y. Jheng, H.-Y. Wang, J.-C. Wu, and A.-Y. Wu, "Traffic-and thermal-aware run-time thermal management scheme for 3D NoC systems," in *Networks-on-Chip (NOCS), 2010 Fourth ACM/IEEE International Symposium on*, 2010, pp. 223–230
[13] R. Cochran and S. Reda, "Consistent runtime thermal prediction and control through workload phase detection," in *Proceedings of the 47th Design Automation Conference*, 2010, pp. 62–67
[14] A. K. Coskun, J. L. Ayala, D. Atienza, T. S. Rosing, and Y. Leblebici, "Dynamic thermal management in 3D multicore architectures," in *Design, Automation & Test in Europe Conference & Exhibition*, 2009, pp. 1410–1415
[15] V. Coropceanu, J. Cornil, D. A. da Silva Filho, Y. Olivier, R. Silbey, and J.-L. Brédas, "Charge transport in organic semiconductors," *Chem. Rev.*, vol. 107, no. 4, pp. 926–952, 2007
[16] A. Facchetti, "Π-conjugated polymers for organic electronics and photovoltaic cell applications†," *Chem. Mater.*, vol. 23, no. 3, pp. 733–758, 2010.
[17] Y. Zhang, J. Zou, H.-L. Yip, K.-S. Chen, D. F. Zeigler, Y. Sun, and A. K.-Y. Jen, "Indacenodithiophene and quinoxaline-based conjugated polymers for highly efficient polymer solar cells," *Chem. Mater.*, vol. 23, no. 9, pp. 2289–2291, 2011.
[18] R. Noriega, J. Rivnay, K. Vandewal, F. P. V Koch, N. Stingelin, P. Smith, M. F. Toney, and A. Salleo, "A general relationship between disorder, aggregation and charge transport in conjugated polymers," *Nat. Mater.*, 2013.
[19] L. H. Sperling, *Introduction to physical polymer science*. John Wiley & Sons, 2005
[20] S. Shen, A. Henry, J. Tong, R. Zheng, and G. Chen, "Polyethylene nanofibres with very high thermal conductivities," *Nat. Nanotechnol.*, vol. 5, no. 4, pp. 251–255, 2010.
[21] R. Y. Wang, R. A. Segalman, and A. Majumdar, "Room temperature thermal conductance of alkanedithiol self-assembled monolayers," *Appl. Phys. Lett.*, vol. 89, no. 17, p. 173113, 2006
[22] E. W. Bentilla, K. F. Sterrett, and L. E. Karre, "Research and development study on thermal control by use of fusible materials," *NASA Tech. Report) Northrop Sp. Lab. Contract No. NAS*, pp. 8–11163, 1966
[23] W. R. Humphries and E. I. Griggs, "A design handbook for phase change thermal control and energy storage devices," *NASA STI/Recon Tech. Rep. N*, vol. 78, p. 15434, 1977
[24] A. Sharma, V. V Tyagi, C. R. Chen, and D. Buddhi, "Review on thermal energy storage with phase change materials and applications," *Renew. Sustain. energy Rev.*, vol. 13, no. 2, pp. 318–345, 2009
[25] R. Chebi P. A. Rice, and J. A. Schwarz, "Heat dissipation in microelectronic systems using phase change materials with natural convection," *Chem. Eng. Commun.*, vol. 69, no. 1, pp. 1–12, 1988.
[26] D. Pal and Y. K. Joshi, "Application of phase change materials to thermal control of electronic modules: a computational study," *J. Electron. Packag.*, vol. 119, no. 1, pp. 40–50, 1997
[27] V. Shanmugasundaram, J. R. Brown, and K. L. Yerkes, "Thermal management of high heat-flux sources using phase change materials: a design optimization procedure," in *Proceedings of the 32nd AIAA Thermophysics Conference, AIAA-1997-2451*, 1997
[28] D. L. Vrable and K. L. Yerkes, "A thermal management concept for more electric aircraft power system applications," SAE Technical Paper, 1998
[29] D. Pal and Y. K. Joshi, "Thermal management of an avionics module using solid-liquid phase-change materials," *J. Thermophys. heat Transf.*, vol. 12, no. 2, pp. 256–262, 1998
[30] E. M. Alawadhi and C. H. Amon, "PCM thermal control unit for portable electronic devices: experimental and

Copyright © 2015 by ASME

numerical studies," *Components Packag. Technol. IEEE Trans.*, vol. 26, no. 1, pp. 116–125, 2003
[31] M. J. Vesligaj and C. H. Amon, "Transient thermal management of temperature fluctuations during time varying workloads on portable electronics," *Components Packag. Technol. IEEE Trans.*, vol. 22, no. 4, pp. 541–550, 1999
[32] R. A. Wirtz, N. Zheng, and D. Chandra, "Thermal management using' dry' phase change material," in *Semiconductor Thermal Measurement and Management Symposium, 1999. Fifteenth Annual IEEE*, 1999, pp. 74–82
[33] M. Hodes, R. D. Weinstein, S. J. Pence, J. M. Piccini, L. Manzione, and C. Chen, "Transient Thermal Management of a Handset Using Phase Change Material (PCM)," *J. Electron. Packag.*, vol. 124, no. December 2002, p. 419, 2002
[34] S. P. Gurrum, Y. K. Joshi, and J. Kim, "Thermal management of high temperature pulsed electronics using metallic phase change materials," *Numer. Heat Transf. Part A Appl.*, vol. 42, no. 8, pp. 777–790, 2002
[35] Z. Luo, H. Cho, X. Luo, and K. Cho, "System thermal analysis for mobile phone," *Appl. Therm. Eng.*, vol. 28, no. 14, pp. 1889–1895, 2008
[36] F. L. Tan and C. P. Tso, "Cooling of mobile electronic devices using phase change materials," *Appl. Therm. Eng.*, vol. 24, no. 2, pp. 159–169, 2004
[37] A. Raghavan, Y. Luo, A. Chandawalla, M. Papaefthymiou, K. P. Pipe, T. F. Wenisch, and M. M. K. Martin, "Computational sprinting," in *High Performance Computer Architecture (HPCA), 2012 IEEE 18th International Symposium on*, 2012, pp. 1–12
[38] L. Shao, A. Raghavan, L. Emurian, M. C. Papaefthymiou, T. F. Wenisch, M. M. K. Martin, and K. P. Pipe, "On-chip Phase Change Heat Sinks Designed for Computational Sprinting," 2014
[39] F. Sarvar, D. C. Whalley, and P. P. Conway, "Thermal interface materials-A review of the state of the art," in *Electronics Systemintegration Technology Conference, 2006. 1st*, 2006, vol. 2, pp. 1292–1302
[40] ASTM D5470-12, Standard Test Method for Thermal Transmission Properties of Thermally Conductive Electrical Insulation Materials, ASTM International, West Conshohocken, PA, 2012, www.astm.org
[41] A. M. Marconnet, N. Yamamoto, M. A. Panzer, B. L. Wardle, and K. E. Goodson, "Thermal Conduction in Aligned Carbon Nanotube–Polymer Nanocomposites with High Packing Density," *ACS Nano*, vol. 5, no. 6, pp. 4818–4825, Jun. 2011
[42] M. T. Barako, Y. Gao, Y. Won, A. M. Marconnet, M. Asheghi, and K. E. Goodson, "Reactive Metal Bonding of Carbon Nanotube Arrays for Thermal Interface Applications," *Components, Packaging and Manufacturing Technology, IEEE Transactions on*, vol. 4, no. 12. pp. 1906–1913, 2014
[43] M. T. Barako, W. Park, A. M. Marconnet, M. Asheghi, and K. E. Goodson, "Thermal Cycling, Mechanical Degradation, and the Effective Figure of Merit of a Thermoelectric Module," *J. Electron. Mater.*, vol. 42, no. 3, pp. 372–381, Dec. 2012
[44] D. Court, "Reliability Report THERMFLOW ™ T766 Reliability Test Report T766 Reliability Report," pp. 1–16

Copyright © 2015 by ASME